T. Zaharia, A. W. Kleyn and M. A. Gleeson (2014). "Eley-Rideal Reactions with N Atoms at Ru(0001): Formation of NO and N2." Physical Review Letters **113**(5): 053201.
DOI: 10.1103/PhysRevLett.113.053201

Eley-Rideal reactions with N atoms at Ru(0001): Formation of NO and N_2

Teodor Zaharia[1,2], Aart W. Kleyn[2,3,*], Michael A. Gleeson[2,†]

[1] Materials innovation institute (M2i), P.O. Box 5008, 2600 GA Delft, The Netherlands

[2] FOM Institute DIFFER (Dutch Institute For Fundamental Energy Research), P.O. Box 1207, 3430 BE Nieuwegein, The Netherlands

[3] Van 't Hoff Institute for Molecular Sciences, Faculty of Science, P.O. Box 94157, 1090 GD Amsterdam, University of Amsterdam, The Netherlands

Abstract

Forward-directed NO molecules with large translational energies are formed upon exposure of an O-covered Ru(0001) surface to a nitrogen ($N+N_2$) beam. This is an unequivocal experimental demonstration of Eley-Rideal reaction for a 'heavy' (i.e. non-hydrogenated) neutral system. The time dependence of prompt NO formation exhibits an exceptionally fast decay as a consequence of shifting reaction pathways and probabilities over the course of the exposure. Prompt production shuts down as the O coverage decreases due to competition from more favourable Eley-Rideal production of N_2.

Keywords: Eley-Rideal reaction, hyperthermal, molecular beam, surface scattering, energy transfer, reaction cross-section.

[*] Present address: Center of Interface Dynamics for Sustainability, Chengdu Development Center for Science and Technology, Chengdu, Sichuan 610207, People's Republic of China.
[†] Corresponding author: m.a.gleeson@differ.nl

T. Zaharia, A. W. Kleyn and M. A. Gleeson (2014). "Eley-Rideal Reactions with N Atoms at Ru(0001): Formation of NO and N2."
Physical Review Letters **113**(5): 053201.
DOI: 10.1103/PhysRevLett.113.053201

Chemical reactions at solid surfaces are the basis of heterogeneous catalysis. Surface reactions take place preferentially because bonds that are very stable in the gas phase can be more easily broken. There are two proto-typical mechanisms: Langmuir-Hinshelwood (LH) and Eley-Rideal (ER)[1, 2]. In LH processes, all reactants first adsorb at the surface, bonds are broken and new bonds formed, and finally the product leaves – typically directed along the surface normal. The essence is a complete decoupling of initial reactant adsorption from final product formation: all "memory" of the pre-adsorption energy and momentum is lost. Diffusion of species over the surface is essential, the residence time at the surface is long, and reaction rates have a strong surface temperature dependence. In contrast, ER reactions involve an incident projectile directly abstracting an adsorbate from the surface. The reaction proceeds promptly - as in a single collision - irrespective of surface temperature[2-6]. The projectile kinetic energy and potential energy gained by entering a deep chemisorption well allows reaction at low temperatures. The overall process is exothermic because the energy of the projectile is not dissipated at the surface. While energy may be needed to prevent a projectile–surface bond from forming, it is usually gained during molecular bond formation and repulsion of the molecule from the surface. In this way the often strong adsorbate-surface bond can be broken. The final trajectory of the product is determined by the combination of its - typically repulsive - interaction with the surface and the retention of momentum from the original projectile.

The LH mechanism is the quintessential mechanism of standard chemistry, while the ER mechanism comes to the fore under more exotic conditions such as plasma environments. Examples include spacecraft re-entry, where ER-reactions lead to materials degradation and glow phenomena[7, 8], and radical interactions with extreme ultraviolet lithography optics[9, 10]. In practice LH and ER represent extremes on a reaction continuum. An important "intermediate" is the hot atom (HA) reaction[11]. In this case the projectile does not transfer its kinetic and potential energy to the surface but does enter a quasi-bound state. HA reactions can typically be regarded as close to ER reactions, but may be sub-divided into *meta-stable* and *bound*

processes[12, 13]. The distinction between a prompt ER and a meta-stable HA reaction can often only be made in computer simulations[6].

Characteristics of ER reactions are the formation of fast products with internal excitation and partial retention of parallel momentum of the projectile in the product[14, 15]. Energy retention is a condition most easily fulfilled by light atoms, which have a poor energy accommodation at surfaces[5]. Consequently, most ER-like reactions studied experimentally have involved hydrogen atoms. Key reactions include formation of H_2 and HCl upon incidence of atomic H[4, 16]. ER reactions have also been reported for fast ions. However, these are far from standard catalytic conditions and the reactions are endothermic[17, 18]. Electrostatic interactions play a dominant role in these cases. In the case of O_2^- formation in a collision of O^+ with O atoms adsorbed at Si(100)[18], the reaction threshold of around 20 eV suggests a kind of direct recoiling of O_{ads} by O_{fast} rather than a pure chemical reaction. Pickup of an H-atom by fast $N(C_2H_4)_3N$ molecules also cannot be considered a regular chemical reaction[19].

No definitive experimental observations of ER reactions involving neutral 'heavy' atoms reacting with adsorbed atoms of similar mass have been reported. Theoretical predictions are made for ER reactions in the N/N-W(100) system[6, 13], but experimental verification is unavailable. One of the closest examples to date is the indication of N-abstraction of N from Ag(111)[20]. While the presence of a large N_2 component in the incident beam precludes definitive assignment on the sole basis of the measurements, molecular dynamics (MD) simulations validate the inference of an ER reaction[21]. A similar issue affects attribution of a possible ER process in the case of hyperthermal O interaction with graphite[22]. The desire for definitive experimental demonstration prompted the work in this paper. We observe ER reactions during exposure of O-covered Ru(0001) to a beam of nitrogen atoms and molecules. Ejection of translationally-hot NO is detected along the forward direction of the collision plane at an angle of about half the projectile specular scattering angle. The measured N_2 signal is initially attenuated, but it increases as O is reacted off. The time dependent behaviour of the

system is consistent with strong suppression of the N-O ER process as a competing N-N reaction becomes available.

The experimental setup and methods have been described elsewhere[23-25]. The sample was a Ru crystal, oriented to <0.1° of the (0001) face. O-covered Ru was prepared by background dosing of O_2 at a pressure of ~2×10^{-8} mbar and a sample temperature (T_s) of 600 K for 600 s (~9 L exposure). Due to the self-limiting nature of the oxygen overlayers this leads to a "saturation" coverage of 0.5 ML, corresponding to an Ru(0001)-O(2×1) structure[26]. This was exposed to a high-temperature effusive beam comprised of an approximately equal mixture of N and N_2 species, with average energies ($\langle E \rangle$) in the range of 4-6 eV[27]. The normal incidence N-atom flux is estimated at ~6.6×10^{14} at·cm^{-2}·s^{-1}. Unless otherwise stated, the exposures were done at T_s=600 K. The main diagnostic tool was a quadrupole mass spectrometer (QMS) that could be moved around the sample to detect particles leaving from the surface along the scattering plane. The azimuthal orientation of the incident beam was along the close-packed atomic rows. Incident (θ_i) and outgoing (θ_f) angles are referenced to the surface normal. The angular acceptance of the detector was ~2°. Out-of-plane production of NO is highly likely, but cannot be detected in the present set up.

Two types of measurements are used in this work: time-of-flight (TOF) and full beam mode. Measurements in TOF-mode involve mechanical chopping of the beam (eight-slit chopper). In this mode the transmission was 2% of the full beam, thus the flux was strongly attenuated. All particle energies and angular flux intensity distributions presented in this paper were derived from TOF measurements. Energy determination is based on flight time from the chopper to the detector. In the case of simple scattering, measurements are directly referenced to the corresponding direct beam[28]. The analysis of displaced or reaction products is more complex. The flight time of the "parent" species is interpolated to the sample surface and the remaining flight time is attributed to the detected species[25]. Zero surface residence time is assumed. If this is incorrect, it implies a shorter product flight time (i.e. an increase in its energy). Full beam measurements involved monitoring the QMS response of selected masses as a function of

time during exposure to the un-chopped beam. The QMS is placed behind the sample for these measurements. Thus, direct scattering from the sample to the analyser is not possible: the signals acquired represent partial pressure responses.

Figure 1 shows polar plots of NO angular intensity distributions produced when Ru(0001)-O(2×1) is exposed to the nitrogen beam at θ_i=50°, 60°, and 70°. The absence of a clear dependence of θ_f on θ_i is indicative of an interaction at the surface that is more complex than that of simple scattering. The distributions are sharp and forward-peaked with peak intensities at θ_f~25°-30°. These are characteristic signatures of an ER reaction.

It is useful to note the various binding energies for this system: N-Ru~5.6 eV[29, 30]; O-Ru~5.5 eV[30]; N-O~6.5 eV; N-N~9.8 eV. These imply that ER formation of NO by incident N-atoms can be exothermic by up to ~1 eV. In contrast, a LH reaction would be endothermic by ~4.6 eV. An example of the energy profile of NO produced during TOF-mode exposure of the O-Ru surface is shown in Figure 2. This distribution has $\langle E \rangle$~4.5 eV. Such a large translational energy cannot be produced by a LH process. It is comparable to the average energy of the incident N-atom distribution (also shown; $\langle E \rangle$~4.1 eV). The salient features of this comparison are that NO molecules with energies <1 eV are absent, the energy at peak intensity of NO is ~1.4 eV higher than that of the N, and that the NO does not exhibit the same high energy “tail” as the N distribution. The former two points are entirely consistent with a prompt, exothermic ER reaction. The latter indicates an energy-dependent reaction probability, leading to suppression of direct reaction in the case of the highest energy N atoms. MD simulations of N abstraction of N from Ag(111) have found a significant energy dependence, with the reaction probability decreasing at higher incident energies[21].

The NO intensity drops rapidly during TOF measurements; a time-correlated signal is barely detectable after ~180s of exposure in this mode. The change in integrated NO intensity during TOF exposure at θ_i=60°; θ_f=25° is presented in the inset of Figure 2. It exhibits an exponential decrease with a characteristic decay time (τ) of ~45 s. Since an ER reaction represents a

direct collision it can be meaningful to define a cross section (σ) for the process. An NO production cross section can be calculated on the basis of:

$$I_{NO}=ke^{-\sigma\cdot\Phi_{60}\cdot\tau}$$

where *k* is a constant and Φ_{60} is the N-atom flux at θ_i=60°. For the chopped beam, $\Phi_{60}\approx 0.02\times\cos(60°)\times 6.6\times10^{14}$ at·cm^{-2}·s^{-1}. The 1/e value leads to σ≈34 Å^2. This is an exceptionally high value. It is much larger than is typically observed for strongly-bound systems. In some ER-reactions involving hydrogen values of more than 1 Å^2 have been observed[5]. N/N-W(100) calculations[6] yielded values of less than 0.5 Å^2. MD simulations in the case of N/N-Ag(111) do indicate large cross sections, but still limited to the 2.5-4.5 Å^2 range[21]. While experimentally-determined ER cross sections are usually small relative to the surface unit cell area, modelling efforts tend to reveal them as over-estimates. This is often due to the relative importance of meta-stable HA processes, which can be an order of magnitude larger than the ER process[6]. The efficiency of such “side” reactions is one of the reasons that ER processes are generally less prevalent than might be anticipated, *a priori*.

Comparing the derived cross section to the O-Ru unit cell area (~12.7 Å^2) presents a conundrum. While it is conceivable that an isolated O-adatom could exhibit a reaction cross section larger than the O-Ru unit cell area, such a determination should never arise from experimental measurements on the saturated surface because the cross sections of neighbouring atoms would overlap. The reason for the large apparent value is that it does not represent a simple measure of O removal. This is illustrated by the fact that, even if the initial abstraction probability by N atoms were unity, the exponential decay in combination with the incident flux implies that only ~37% of the O adatoms would be removed during the 180s TOF exposure. Since the absence of a high energy NO tail in Figure 2 demonstrates that the reaction probability is not unity, the actual percentage removed is lower.

That the disappearance of the time-correlated signal is not related to complete removal of O was verified by full beam exposures. These also produces an exponentially decaying NO

signal as illustrated in Figure 3(a), which shows two consecutive exposures of the initially saturated O-Ru surface to the full beam. The NO response during these exposures is mirrored in the N_2 response. During the first opening, the N_2 signal increases gradually as the NO signal decays. These responses are associated with the presence of oxygen on the surface. When the beam flag is briefly closed and reopened, the N_2 signal response from the now largely N-covered surface is almost a step function. (The chamber response time is 3-4s.) We attribute the residual NO plateau during the second opening to a chamber effect.

The same qualitative behaviour is observed during full beam exposure of an O-Ru surface that was first exposed in TOF-mode for 180s (nominally equivalent to 3.6s of full beam exposure). The main difference is in the magnitude of the initial NO (Figure 3(b)) and corresponding N_2 responses. The N_2 responses can be inverted to produce "missing" N_2 signals (Figure 3(c)) by subtracting the response during the first flag opening from that during the second. The origin of this "missing" signal is N_2 formation by reaction of incident N with N adatoms. This cannot occur on the initial surface, but emerges as the surface becomes progressively more N-covered, which is due to direct adsorption of N atoms from the incident beam.

The difference in integrated areas between the full beam responses with and without a pre-TOF exposure is a measure of the surface changes occurring while the NO ER process is active. In the case of the NO signal (Figure 3(b)) the difference indicates an ~20% decrease due to the 180 seconds TOF exposure, allowing us to put an absolute value on the number of O atoms that are readily removed by prompt processes (~1.6×10^{14} cm^{-2} as compared with the initial Ru(0001)-O(2×1) O-atom density ~7.9×10^{14} at./cm^2). The decay curve shown in Figure 2 represents the in-plane formation rate of prompt NO, which should be equivalent to the O-removal rate. Hence, the integrated area under the curve is proportional to the total number of O atoms removed provided that prompt NO ejected in-plane is proportional to total prompt NO production (in- and out-of-plane). We note that if the relative amount of in-plane NO being

produced is decreasing over the course of the TOF-mode measurement, then this would be a contributing factor in the observed rapid signal decay.

Provided in-plane production is indeed proportional to total NO production, then the initial O-reaction probability is ~54%. Under an assumption of non-varying N trajectories, this translates to a cross section of ~6.9 $Å^2$ (relating reaction probability to unit cell area). Accounting for the surface shadowing effect due to the angle of incidence, the corresponding normal incidence cross section would be ~4.6 $Å^2$. While still remarkably large, these values are more consistent with abstraction from a saturated surface.

In the case of the "missing N_2" signal (Figure 3(c)) the difference between the exposures is ~33%. Thus, the surface already attains ~$^1/_3$ of its steady-state N-coverage during the TOF exposure. While the nominal saturation coverage of N-Ru(0001) at T_s<400 K is 1 ML, at the current exposure temperature (600 K) the maximum coverage attainable is ≤0.5 ML[31]. N-N reaction to form N_2 will tend to suppress the steady-state coverage. Thus, at most every O adatom will be replaced by one N adatom. The N_2 response attains its plateau level after ~50s of exposure, while O removal is still on-going. This disparity is related to the fact that at least half of the potential N-adsorption sites on the Ru(0001)-O(2×1) surface are initially vacant. Thus the steady-state N-coverage can be established without requiring complete O-removal.

There is a dramatic difference between the magnitudes of the NO and N_2 responses in both cases shown in Figure 3(b)&(c). The decreasing NO signals coincide with an increase in the N_2 signal that is on average ~11 times larger. The correlation between the two responses is not constant in time. The response factor decreases from ~16 to ~8 during the first 50s of full beam exposure. The electron impact ionization cross sections of NO and N_2 are comparable (NO=2.807 $Å^2$ and N_2=2.508 $Å^2$ at 70 eV[32]), as presumably are the selection and transmission by the QMS. Consequently the response factor indicates that formation of N_2 is strongly favoured when N atoms interact with an intermixed N-/O-Ru surface.

Figure 4 illustrates that a large fraction of N atoms incident on an N-Ru surface are converted to N_2. It shows N and N_2 angular intensity distributions formed by the nitrogen beam incident at θ_i=60°. In this case T_s=400 K, so the standing coverage of N can be higher than that attained during the full beam exposures of the O-Ru surface (T_s=600 K). While the composition of the incident beam is approximately equal in N and N_2, the distributions leaving the surface are heavily weighted in favour of N_2. The N_2 distribution is clearly bi-modal. Comparison with the NO distribution produced by the O-Ru provides strong evidence that the N_2 component at small θ_f is the result of a prompt abstraction reaction. This is supported by the correspondence between the energy distributions of incident N and abstracted N_2 at small θ_f, which is similar to that shown in Figure 2 for N and NO.

We can now account for the rapid disappearance of prompt NO formation in terms of the changing nature of the surface as a function of exposure. The picture that emerges is one of efficient ER abstraction of O adatoms by incident N being superseded by a more favourable production of N_2 as the surface composition changes. Starting from the Ru(0001)-O(2×1) structure, the incident N atoms can scatter, adsorb, or abstract O adatoms. The greatest probability of NO formation is during the initial stages of the exposure. Each O adatom removed opens up an additional potential N adsorption site. With increasing N adsorption the range of interaction possibilities expands to include N_2 formation by an ER reaction. Figure 3 illustrates that this reaction is strongly favored and confirms that the rapid decay of the NO TOF signal does not represent complete removal of O. The apparent 34 $Å^2$ reaction cross section is a consequence of shutting down of the prompt abstraction process due to the emergence of the preferred N-N reaction. The remaining O adatoms continue to be removed at a slow rate, either via low probability ER reaction or via surface-mediated processes. In isolation, the interaction of N with adsorbed O is clearly very attractive in nature. The fact that prompt O abstraction is suppressed implies that the N-N interaction has a significantly longer attractive range and/or larger ER cross section than the corresponding N-O interaction, resulting in an appreciable shielding effect.

In conclusion, definitive experimental evidence of ER reactions between non-hydrogenic reactants has been observed, in spite of the more efficient energy transfer to the lattice associated with heavy atoms. The results also demonstrate the ability of competing reaction pathways to shut down an otherwise favourable ER process. As the O coverage decreases and the co-adsorbed N coverage increases, prompt NO production is rapidly attenuated because the reaction probability of incident N is significantly higher with N than with O adatoms.

Acknowledgements

This research was carried out under the project number M61.3.11431 in the framework of the Research Program of the Materials innovation institute (M2i). The authors would like to thank Arend-Jan van Calcar for skilful technical assistance with the experimental set-up.

T. Zaharia, A. W. Kleyn and M. A. Gleeson (2014). "Eley-Rideal Reactions with N Atoms at Ru(0001): Formation of NO and N2."
Physical Review Letters **113**(5): 053201.
DOI: 10.1103/PhysRevLett.113.053201

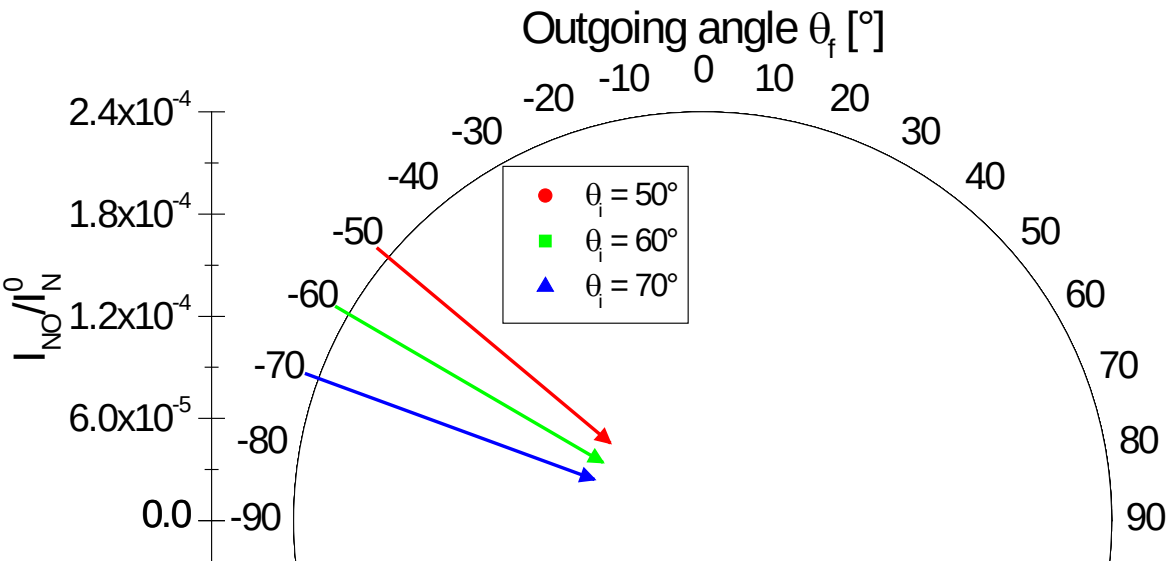

Figure 1: NO angular intensity distributions produced by the nitrogen beam incident on Ru(0001)-O(2×1) at θ_i=50° (circles), 60° (squares), and 70° (triangles). Intensities are normalized to the N atom intensity of the incident beam. Data points are fitted with a shifted cosine functions to the power of ~8.2, ~7, and ~7, respectively. The dashed line is a normal cosine distribution. This function has been scaled to match the integrated area of the cosine fit to the θ_i=60° data.

T. Zaharia, A. W. Kleyn and M. A. Gleeson (2014). "Eley-Rideal Reactions with N Atoms at Ru(0001): Formation of NO and N2."
Physical Review Letters **113**(5): 053201.
DOI: 10.1103/PhysRevLett.113.053201

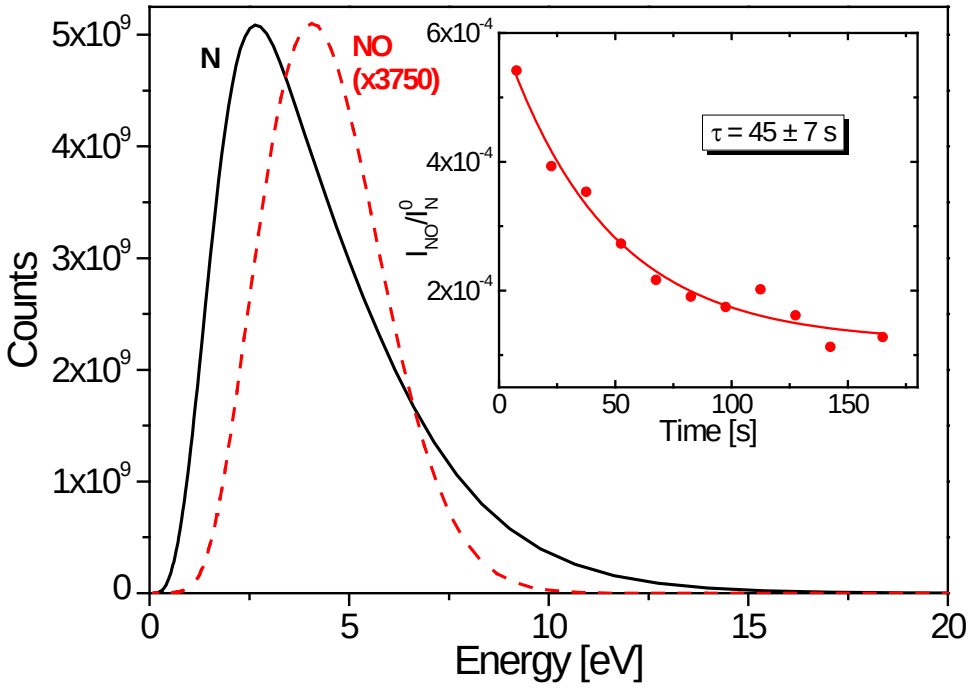

Figure 2: Energy profiles of N atoms in the incident beam (solid line), and NO molecules formed during nitrogen beam exposure of Ru(0001)-O(2×1) at θ_i=60°, θ_f=25° in TOF mode (dashed line; note the scaling factor). **Inset:** Time dependency of the NO TOF integrated area at θ_i=60°, θ_f=25°. The solid line is a single exponential decay fitted to the data.

T. Zaharia, A. W. Kleyn and M. A. Gleeson (2014). "Eley-Rideal Reactions with N Atoms at Ru(0001): Formation of NO and N2."
Physical Review Letters **113**(5): 053201.
DOI: 10.1103/PhysRevLett.113.053201

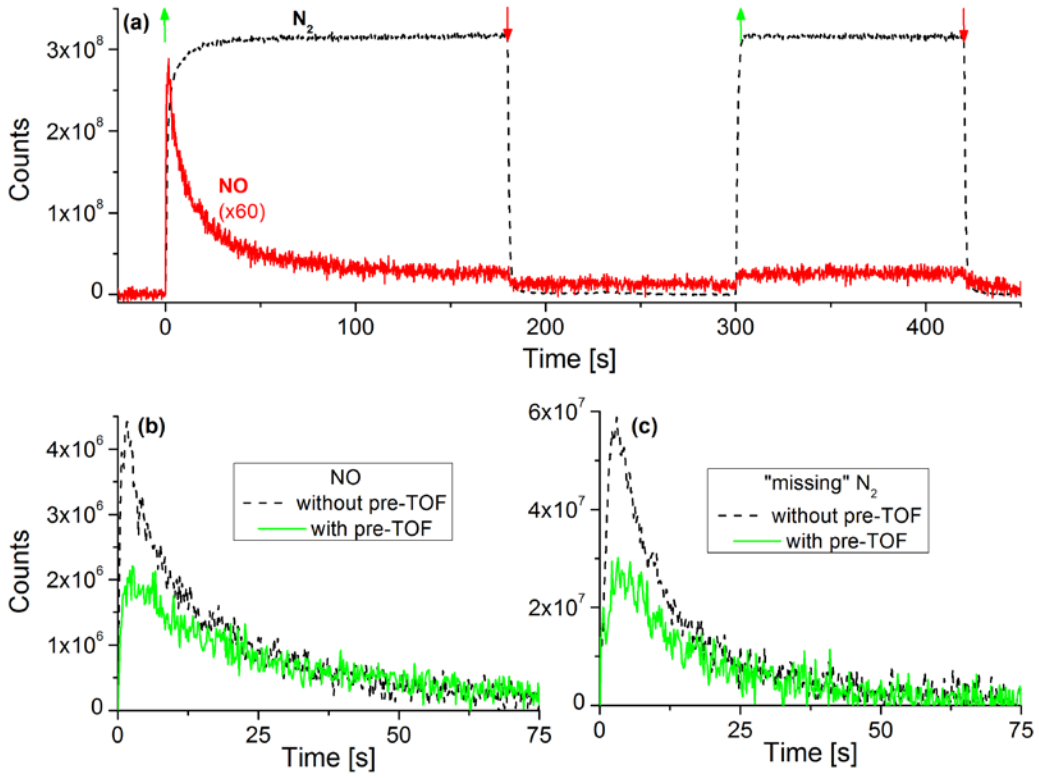

Figure 3: (a) Comparison of QMS m/z=28 (N_2; dashed) and m/z=30 (NO; solid; note the scaling factor) responses during two sequential full beam exposures of an initial Ru(0001)-O(2×1) surface (θ_i=60°). The up and down arrows indicate beam flag openings and closings, respectively. **(b)** Initial NO response during full beam exposure of as-prepared Ru(0001)-O(2×1) (dashed) and the O-Ru surface after a 180s TOF exposure (solid). **(c)** Corresponding "missing" N_2 signals derived from the N_2 responses during full beam exposure.

T. Zaharia, A. W. Kleyn and M. A. Gleeson (2014). "Eley-Rideal Reactions with N Atoms at Ru(0001): Formation of NO and N2."
Physical Review Letters **113**(5): 053201.
DOI: 10.1103/PhysRevLett.113.053201

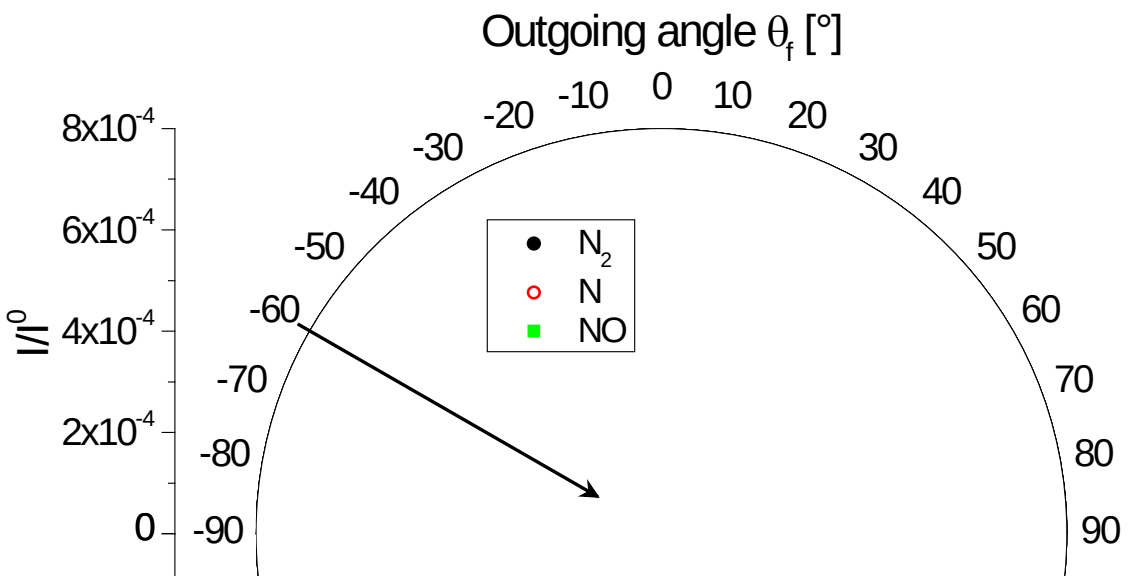

Figure 4: N_2 (filled circles) and N (open circles) angular intensity distributions formed by the nitrogen beam incident on an N-Ru surface at θ_i=60°. The NO distribution at θ_i=60° from Figure 1 (squares) is reproduced. The lines are to guide the eye.

References

1. D. D. Eley and E. K. Rideal, Nature **146** (3699), 401 (1940).
2. A. W. Kleyn, Chem. Soc. Rev. **32** (2), 87 (2003).
3. C. T. Rettner and D. J. Auerbach, Surf. Sci. **358** (1-3), 602 (1996).
4. C. T. Rettner and D. J. Auerbach, Science **263** (5145), 365 (1994).
5. B. Jackson, in *Surface Dynamics*, edited by D. P. Woodruff (Elsevier, Amsterdam, 2003), Vol. 11, pp. 52-77.
6. E. Quintas-Sánchez, P. Larrégaray, C. Crespos, L. Martin-Gondre, J. Rubayo-Soneira and J-C. Rayez, J. Chem. Phys. **137** (6), 064709 (2012).
7. E. Murad, J. Spacecraft Rockets **33** (1), 131 (1996).
8. E. Murad, Annu. Rev. Phys. Chem. **49**, 73 (1998).
9. S. Bajt, N. V. Edwards and T. E. Madey, Surf. Sci. Rep. **63** (2), 73 (2008).
10. S. M. Zyryanov, A. S. Kovalev, D. V. Lopaev, E. M. Malykhin, A. T. Rakhimov, T. V. Rakhimova, K. N. Koshelev and V. M. Krivtsun, Plasma Phys. Rep. **37** (10), 881 (2011).
11. J. Harris and B. Kasemo, Surf. Sci. **105**, L281 (1981).
12. R. Martinazzo, S. Assoni, G. Marinoni and G. F. Tantardini, J. Chem. Phys. **120** (18), 8761 (2004).
13. E. Quintas-Sánchez, C. Crespos, P. Larrégaray, J-C. Rayez, L. Martin-Gondre and J. Rubayo-Soneira, J. Chem. Phys. **138** (2), 024706 (2013).
14. C. T. Rettner and D. J. Auerbach, Phys. Rev. Lett. **74** (22), 4551 (1995).
15. C. T. Rettner, J. Chem. Phys. **101** (2), 1529 (1994).
16. C. T. Rettner, Phys. Rev. Lett. **69** (2), 383 (1992).
17. M. Maazouz, T. L. O. Barstis, P. L. Maazouz and D. C. Jacobs, Phys. Rev. Lett. **84** (6), 1331 (2000).
18. C. L. Quinteros, T. Tzvetkov and D. C. Jacobs, J. Chem. Phys. **113** (13), 5119 (2000).
19. E. W. Kuipers, A. Vardi, A. Danon and A. Amirav, Phys. Rev. Lett. **66** (1), 116 (1991).
20. H. Ueta, M. A. Gleeson and A. W. Kleyn, J. Chem. Phys. **135** (7), 074702 (2011).
21. M. Blanco-Rey, E. Díaz, G. A. Bocan, R. Diéz Muiño, M. Alducin and J. I. Juaristi, J. Phys. Chem. Lett. **4** (21), 3704 (2013).
22. J. T. Paci, H. P. Upadhyaya, J. Zhang, G. C. Schatz and T. K. Minton, J. Phys. Chem. A **113** (16), 4677 (2009).
23. F. Gou, M. A. Gleeson, J. Villette and A. W. Kleyn, Vacuum **81** (2), 196 (2006).
24. H. Ueta, M. A. Gleeson and A. W. Kleyn, J. Phys. Chem. A **113** (52), 15092 (2009).
25. H. Ueta, M. A. Gleeson and A. W. Kleyn, J. Chem. Phys. **134** (6), 064706 (2011).
26. M. Gsell and D. Menzel, Surf. Sci. **603** (10-12), 1397 (2009).
27. T. Zaharia, H. Ueta, A. W. Kleyn and M. A. Gleeson, Z. Phys. Chem. **227** (9-11), 1511 (2013).
28. H. Ueta, M. A. Gleeson and A. W. Kleyn, J. Chem. Phys. **134** (3), 034704 (2011).
29. S. Schwegmann, A. P. Seitsonen, H. Dietrich, H. Bludau, H. Over, K. Jacobi and G. Ertl, Chem. Phys. Lett. **264** (6), 680 (1997).
30. Y. D. Kim, A. P. Seitsonen, S. Wendt, J. Wang, C. Fan, K. Jacobi, H. Over and G. Ertl, J. Phys. Chem. B **105** (18), 3752 (2001).
31. L. Diekhöner, A. Baurichter, H. Mortensen and A. C. Luntz, J. Chem. Phys. **112** (5), 2507 (2000).
32. NIST Standard Reference Database 107, http://physics.nist.gov/PhysRefData/Ionization/molTable.html, National Institute of Standards and Technology, 2014.